

**© 2017 IEEE. Personal use of this material is permitted. Permission from IEEE must be obtained for all other uses, in any current or future media, including reprinting/republishing this material for advertising or promotional purposes, creating new collective works, for resale or redistribution to servers or lists, or reuse of any copyrighted component of this work in other works.**

# Multi-polarization Reconfigurable Circular Patch Antenna with L-shaped Probes

Wei Lin, *Member, IEEE* and Hang Wong, *Senior Member, IEEE*

**Abstract**—This letter introduces a multi-polarization reconfigurable circular patch antenna with eight L-shaped probes. By adopting the L-probe feeding structure, the reported circular patch antenna is compact, simple and low-profile. It has switchable  $0^\circ$ ,  $+45^\circ$ ,  $90^\circ$  and  $-45^\circ$  linear polarizations and is able to mitigate the polarization mismatch problem in complex wireless channels. This polarization reconfigurability is realized by controlling a set of PIN diodes via a switchable feeding network. Measured results show that the antenna has excellent electrical performance for all operating states. The overlapping impedance bandwidth (when the reflection coefficient  $\leq -10$  dB) is 17.6%, from 2.325 to 2.775 GHz, which covers both the WLAN and ISM bands. The gain is very stable across the entire bandwidth with a 6.1 dBi peak value and the cross polarization levels are low. Moreover, good cardioid-shaped radiation patterns are attained.

**Index Terms**—L-probe feed, patch antenna, PIN diodes, multi polarization reconfigurable antenna, polarization mismatch.

## I. Introduction

With the development of modern communication and sensor systems, wireless channels are becoming more and more complex as the number of users and devices increases. Polarization matching is a crucial factor in the determination of the amount of power captured by receiving antennas in these systems. Communication links will break down if a polarization mismatch transpires. For example, in the wireless sensor network system illustrated in Fig. 1, polarization mismatch will occur if its receiving antenna is single-polarized and random-polarized waves from more than one wireless sensor are incident on it. To address this problem, dual-polarization or multi-polarization antennas have been considered. However, comparing the quality of the output signals resulting from the interactions of random incident

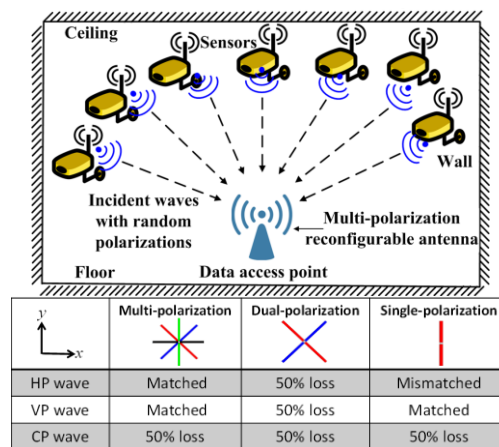


Fig. 1. Complex channels in a wireless sensor network system.

waves with a variety of different receiving antennas, it has been determined that the multi-polarization reconfigurable antenna is the best candidate to mitigate the polarization mismatching problem in such wireless systems. On the other hand, it also has been found that a circularly-polarized antenna is not a good option. It will always suffer from at least a 50% loss when receiving linearly-polarized incident waves. Moreover, serious polarization mismatches will occur if the incident wave has the opposite circular polarization. For example, the polarization states are entirely mismatched when a LHCP antenna receives a RHCP incident wave.

Many linear polarization reconfigurable antennas have been realized and reported. Based on the design of their reconfigurable radiators or feeding networks, the antennas in [1] — [6] have realized orthogonally-switchable polarizations. The designs in [7] and [8] achieved three reconfigurable linear polarizations. However, there is only one reported design to date that can realize four switchable linear polarizations, i.e., as  $0^\circ$ ,  $+45^\circ$ ,  $90^\circ$  and  $-45^\circ$ . This achievement was reported in our previous works [9] and [10]. Unfortunately, there are obvious disadvantages of that design, including its complex structure; a bulky, messy biasing network; and poor overall efficiency.

In this letter, we propose a multi-polarization reconfigurable circular patch antenna which is simple, compact, and low-profile, and exhibits excellent performance characteristics. By adopting the L-probe feeding method and

This work was supported in part by the Research Grants Council of the Hong Kong SAR, China (Project No. CityU138413), in part by the National Science and Technology Major Project under Grant 2015ZX03001006 and Guangdong Joint Innovation Project in Guangdong Province under Grant 2014B050504002.

Wei Lin is with the Global Big Data Technologies Centre, University of Technology Sydney, Sydney, Australia and was with the State Key Laboratory of Millimeter Waves, Department of Electronic Engineering, City University of Hong Kong, Hong Kong SAR, China (E-mail: wei.lin@uts.edu.au)

Hang Wong is with the State Key Laboratory of Millimeter Waves, Department of Electronic Engineering, City University of Hong Kong, Hong Kong SAR, China (E-mail: hang.wong@cityu.edu.hk).

designing an optimal reconfigurable feeding network, the system is able to alter its polarization amongst four states by controlling the PIN diodes. The presence of four additional suspended L-shaped probes is critical to the reduction of the cross polarization levels because of the intrinsic symmetry of the structure. Compared with the first multiple linear polarization reconfigurable antenna [9], the diameter and height of the reported design have been reduced by 46% and 65%, respectively. Furthermore, the cross polarization levels have been improved by around 10 dB.

## II. Antenna Design

### A. Antenna Configuration

The antenna consists of three main parts as shown in Fig. 2: A top circular radiating patch; a reconfigurable feeding network connected with eight L-shaped probes; and an additional substrate for the DC biasing lines. In order to ensure symmetry for the four polarization states, a circular patch was adopted as the radiating element instead of the traditional rectangular choice. Its radius and its height above the ground plane are  $R_{patch}$  and  $H_{patch}$ , respectively. An output port reconfigurable feeding network is etched on Substrate#1\_Feeding, which is the surface located below the patch. It controls the selection of which port amongst the four output ports that will be excited. We introduce and control a set of PIN diodes located between the transmission lines of this feeding network to realize the desired reconfigurability. To excite the radiating circular patch, eight L-shaped probes are evenly distributed below it. The radius of the vertical parts of the L-probes from the centre is represented by the radius  $R_{probe}$ . The four feeding probes, P#1 to P#4, are connected to the four output ports of the feeding network. The other four probes are suspended without connecting to any metallic object. The reason for adding the four suspended probes will be discussed in detail in Part C. The length and height of each L-probe are defined, respectively, as  $L_{probe}$  and  $H_{probe}$ . There are DC biasing pads fabricated on Substrate#2\_DC, which is placed with a 1.0 mm gap below the Substrate#1\_Feeding. These two substrates have the same radius,  $R_{antenna}$ . Through the indicated metallic posts and RF chokes, DC#1 to DC#4 are DC-connected, but are RF-isolated to P#1 to P#4, respectively. Besides these three main parts, four plastic screws and one 3D-printed fixture are used to mechanically support the patch and the probes respectively. Finally, a SMA connector is fixed at the ground of substrate#1 through the rectangular region removed from Substrate#2\_DC. The key parameter values of the antenna design are (in millimeters):  $R_{patch} = 21.0$ ,  $H_{patch} = 10.0$ ,  $L_{probe} = 23.0$ ,  $H_{probe} = 6.0$ ,  $R_{probe} = 24.5$ ,  $R_{antenna} = 40.0$ .

### B. Switching Mechanism

The arrangement of the PIN diodes is presented in Fig. 3. The Bar50-02L diode from Infineon Technologies was used in

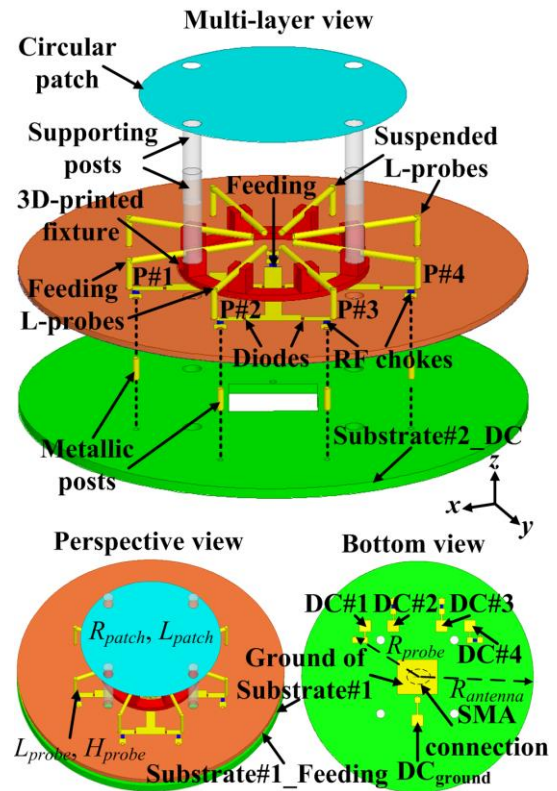


Fig. 2. Antenna configuration.

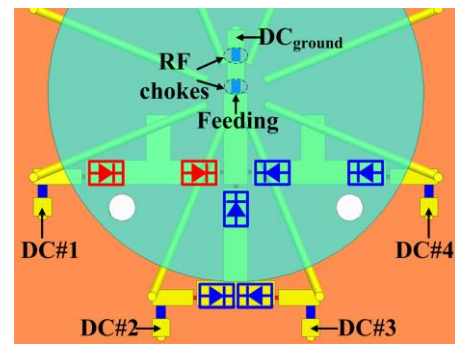


Fig. 3. Arrangement of the PIN diodes (Top view of the antenna).

TABLE I  
POLARIZATION STATES BY STATUS OF THE DC BIASES

DC#1	DC#2	DC#3	DC#4	DC_ground	Polarization mode
3 V	0 V	0 V	0 V	0 V	Mode#1: $0^\circ$
0 V	3 V	0 V	0 V	0 V	Mode#2: $+45^\circ$
0 V	0 V	3 V	0 V	0 V	Mode#3: $90^\circ$
0 V	0 V	0 V	3 V	0 V	Mode#4: $-45^\circ$

all instances in this design. The equivalent circuit model and electrical characteristics of this diode can be found in our previous papers [11] and [12]. By controlling the ON/OFF status of these diodes, one can alter the polarization states as shown in Table I. For example, if we apply a 3.0 V DC bias to DC#1 and a 0 V bias to DC\_ground, the two diodes between probe

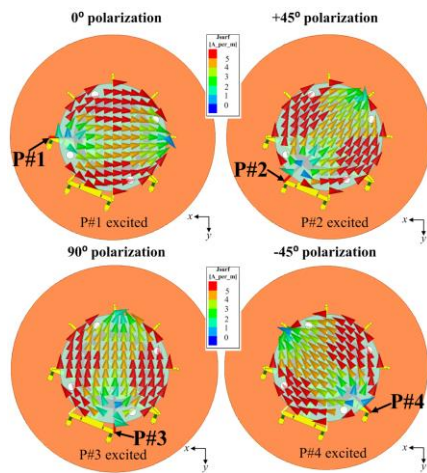


Fig. 4. Current distributions for each polarization state at 2.5 GHz.

P#1 and the first section of the feeding transmission line will be turned on. In contrast, all of the other diodes remain off. In this state, the L-probe P#1 will be excited and the  $0^\circ$  polarization state is generated. Similarly, if the 3.0 V positive voltage bias is switched to any of the other probes, the desired polarization state switching will be realized. Figure 4 exhibits the current distributions on the patch when the different L-probes are excited. We can clearly see that each polarization state corresponds to a particular L-probe excitation.

### C. Design of additional L-probes

Besides the four feeding L-probes, the four suspended probes are critical to the design. As Fig. 5 indicates, the cross polarization patterns are asymmetrical and large when the four suspended L-probes are removed. If the structure were asymmetrical, the strong coupling between the feed probes would significantly deteriorate the radiation patterns (cross polarization level will be increased by 20 dB). In order to keep the symmetry of the entire design and to generate good radiation patterns, the four suspended L-probes are indispensable.

## III. Measured results

A prototype of the optimized antenna was fabricated; it is shown in Fig. 6. The disk for the feed network, substrate#1, is from Wangling Ltd.; it has a 2.65 relative permittivity, a 0.001 loss tangent, and a 1.0 mm thickness. The other disk, substrate#2, for the DC network, is FR4; it has a 1.6 mm thickness. The relative permittivity of the 3D-printed fixture is around 2.95; it has negligible influence on the antenna performance. The antenna was simulated with the Ansoft high frequency structure simulator (HFSS) and was measured in with Starlab SATIMO near-field measurement system.

The measured and simulated reflection coefficients are shown in Fig. 7. It is observed that both the measured and simulated impedance bandwidths agree quite well. The measured impedance bandwidths for all of the operating

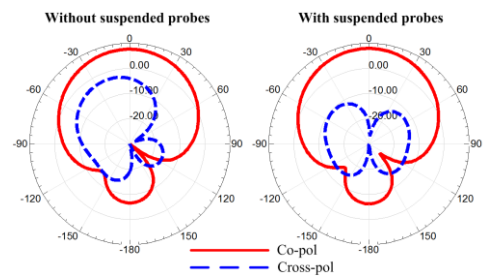


Fig. 5. Simulated radiation patterns with and without the four suspended L-probes at 2.5GHz.

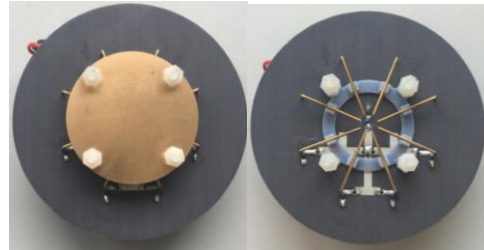


Fig. 6. Fabricated antenna.

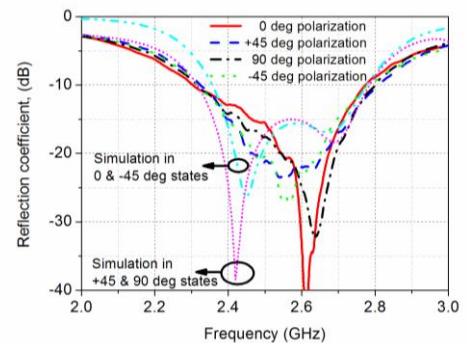


Fig. 7. Measured and simulated reflection coefficient as functions of the source frequency for all of the polarization states.

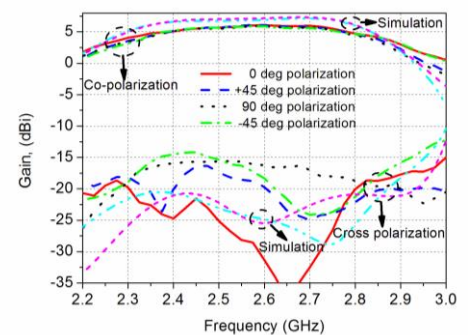


Fig. 8. Measured and simulated gain values as functions of the source frequency for all of the polarization states.

modes are stable and overlap with each other. The measured (simulated) realized impedance bandwidth is 17.6% (16.3%), from 2.33 to 2.78 GHz (from 2.36 to 2.78 GHz). The discrepancies in the measured and simulated resonance frequencies, which are very sensitive to the design parameters, arise from the fabricated differences in the dimensions (heights and lengths) of the L-probes. The resonance point will move to a higher frequency if the length of the L-probe is increased slightly.



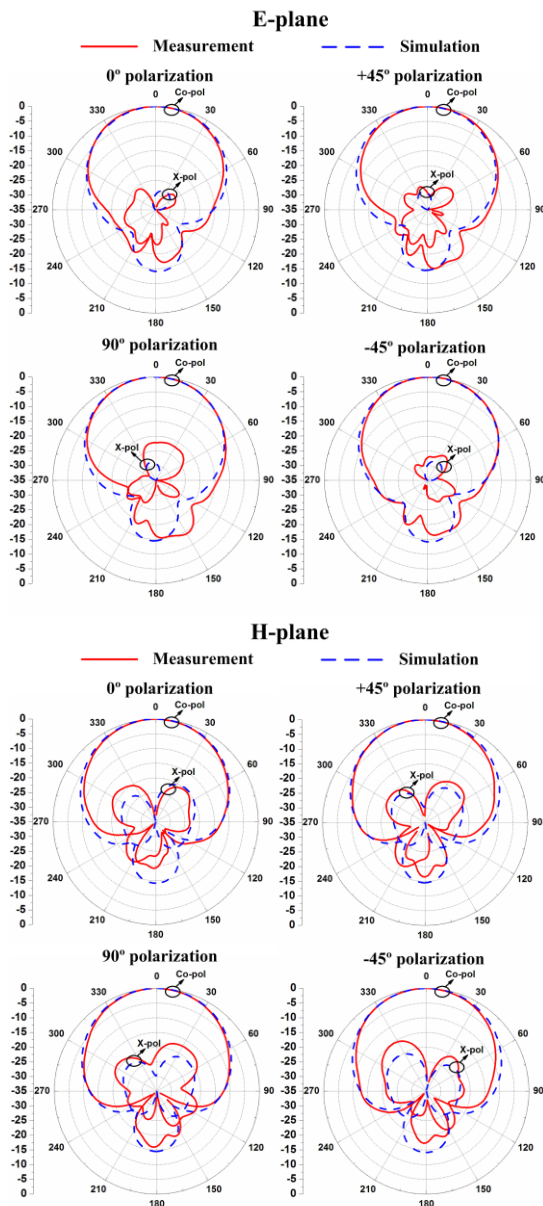


Fig. 9. Measured and simulated radiation patterns in the E- and H- planes for all of the polarization states at 2.5 GHz.

The measured and simulated gain values for all of the polarization states are shown in Fig. 8. The measured gain is stable across the entire operating bandwidth and has a 6.1 dBi peak value. The co-polarization and cross-polarization ratio is larger than 20 dB across this band. The measured gain is 1 dB lower than the simulated values within the bandwidth. This difference is mainly due to the losses from the diodes and the RF chokes. The measured and simulated E- and H-plane radiation patterns for each polarization state at 2.5 GHz are presented in Fig. 9. It is observed that good broadside radiation patterns are realized and the 6.1 dBi peak gain value occurs in the broadside direction with the cross polarization level being lower than -20 dBi. These measured results validate that the

reported reconfigurable antenna has excellent performance characteristics for all four polarization states. In particular, consistent performance was obtained when the polarization states were switched.

#### IV. Conclusion

A polarization reconfigurable antenna with  $0^\circ$ ,  $+45^\circ$ ,  $90^\circ$  and  $-45^\circ$  polarization states was reported. The antenna structure, operating principles, and key design concerns were discussed. The measured results validate the design concepts and agree well with their simulated values. Because this polarization reconfigurable antenna can mitigate the polarization mismatch problems that arise in complex wireless sensor network channels, it has many potential applications.

#### ACKNOWLEDGMENT

The authors would like to thank Prof. Richard Ziolkowski at University of Technology Sydney for his valuable comments and thorough revision of the English writing in this paper.

#### V. References

- [1] W. Lin and H. Wong, "Polarization reconfigurable aperture-fed patch antenna and array," *IEEE Access*, vol. 4, pp. 1510-1517, Apr. 2016.
- [2] T. Song, Y. Lee, D. Ga and J. Choi, "A Polarization Reconfigurable Microstrip Patch Antenna using PIN Diodes," *Proceedings of APMC 2012*, Dec. 4-7, 2012.
- [3] Y. Li, Z. J. Zhang, W. H. Chen and Z. H. Feng, "Polarization reconfigurable slot antenna with a novel compact CPW-to-slotline transition for WLAN application," *IEEE Antenna and wireless propag. letters*, vol. 9, pp. 252-255, 2010.
- [4] K. Boonying, C. Phongcharoenpanich and S. Kosulvit, "Polarization reconfigurable suspended antenna using RF switches and P-I-N diodes," *The 4th Joint International Conference on Information and Communication Technology*, 2014.
- [5] M. S. Nishamol, V. P. Sarin, D. Tony, C. K. Aanandan, P. Mohanan, and K. Vasudevan, "An electronically reconfigurable microstrip antenna with switchable slots for polarization diversity," *IEEE Trans. Antennas Propag.*, vol. 59, no. 9, pp. 3424-3427, Sep., 2011.
- [6] M.H. Amini, H.R. Hassani and S. Mohammad ali nezhad, "A single feed reconfigurable polarization printed monopole antenna," *IEEE 6th European Conference on Antennas and Propagation (EUCAP)*, 2012.
- [7] P. Y. Qin, Y. Guo and C. Ding, "A dual-band polarization reconfigurable antenna for WLAN systems," *IEEE Trans. Antennas Propag.*, vol. 61, no.11, pp. 5706-5713, Nov., 2013.
- [8] P. Y. Qin, Y. Guo, Y. Cai, E. Dutkiewicz and C. H. Liang, "A reconfigurable antenna with frequency and polarization agility," *IEEE Antenna and wireless propag. letters*, vol. 10, pp. 1373-1376, 2011.
- [9] W. Lin and H. Wong, "Polarization reconfigurable multi-slot antenna for body-centric wireless communication system," *IEEE International Workshop on Electromagnetics (IWEM)*, May, 2016.
- [10] H. Wong, W. Lin, L. Huitema and E. Arnaud, "Multi-polarization Reconfigurable Antenna for Wireless Biomedical System," *IEEE Transactions on Biomedical Circuit and System*, accepted in Nov. 2016.
- [11] W. Lin and H. Wong, "Polarization reconfigurable wheel-shaped antenna with conical-beam radiation pattern," *IEEE Transactions on Antennas and Propagation*, vol. 63, no. 2, pp. 491-499, Feb, 2015.
- [12] W. Lin and H. Wong, "Wideband circular polarization reconfigurable antenna," *IEEE Transactions on Antennas and Propagation*, vol. 63, no. 12, pp. 5938-5944, Dec, 2015.